



24th COBEM - 2017



24th ABCM International Congress of Mechanical Engineering  
December 3-8, 2017, Curitiba, PR, Brazil

COBEM-2017-2567

## THERMAL PERFORMANCE OF A HEAT PUMP WITH SOLAR EVAPORATOR IN SUNNY ENVIRONMENTS

**Hélio Augusto Goulart Diniz**

Universidade Federal de Minas Gerais, Mechanical Engineering Department, 31270091, Belo Horizonte, MG, Brazil  
helioufmg@gmail.com

**Fernando Neves Quintino dos Santos**

Centro Federal de Educação Tecnológica de Minas Gerais, Energy Engineering Department, 30510000, Belo Horizonte, MG, Brazil  
fernandonquintino@gmail.com

**Juan Jose Garcia Pabon**

**Ricardo Nicolau Nassar Koury**

**Luiz Machado**

Universidade Federal de Minas Gerais, Mechanical Engineering Department, 31270091, Belo Horizonte, MG, Brazil  
langa\_27@hotmail.com  
koury@demec.ufmg.br  
luizm@ufmg.br

**Abstract.** Heat pumps are good substitutes for electric showers for water heating because of their high coefficient of performance (COP) and low power consumption. In places with high solar irradiance, solar evaporators can be used for better performance. The purpose of this work is to analyze the performance of a direct expansion heat pump assisted with a coaxial condenser and solar evaporator, used to fill a 200 L tank with hot water. For this, a prototype was tested under real summer conditions, for various irradiation conditions. The mean COP was 2.66 with heating capacity of 1093.4 W. There was a strong dependence of the COP with the increase of temperature and irradiation. The use of the solar evaporator in heat pumps has the potential to increase COP, making it justifiable with increased irradiation.

**Keywords:** heat pump, solar evaporator, water heating, R134a, coaxial condenser

### 1. INTRODUCTION

Solar heating water heating systems are an alternative for reducing emissions and energy consumption. According to EPE (2016), residential water heating using solar collector in Brazil will grow thrice in the next 10 years. However, this technology has limitation due to limited sunshine. Heat pumps can operate in spite of this limitation, acting as support to solar collectors (Costa e Silva, 2007) or assisted by solar energy (Buker and Riffat, 2016).

Direct expansion solar assisted heat pumps (DX-SAHP) have the evaporator coupled to a solar collector, where the refrigerant evaporates shortly after expansion. This system is interesting in relation to other SAHP configurations because it has better thermodynamic performance, lower cost, longer life (Li et al., 2007) and allows heat storage (Omojaro and Breilkopf, 2013). Li and Yang (2009) compared different solar water heating technologies to heat 280 L water in Hong Kong weather conditions, and found that DX-SAHP provides second-to-best economic returns, prior only to the solar assisted air-source heat pump.

Literature contains several studies on DX-SAHP using immersed condenser with coefficient of performance (COP) ranging from 2-6 (Li et al., 2007; Anderson et al., 2007; Sun et al., 2015), however few consider the use of coaxial condensers (Scarpa and Tagliafico, 2016). The objective of this work is to evaluate experimentally the thermal performance of a DX-SAHP operating with coaxial condenser, for heating 200 L of water.

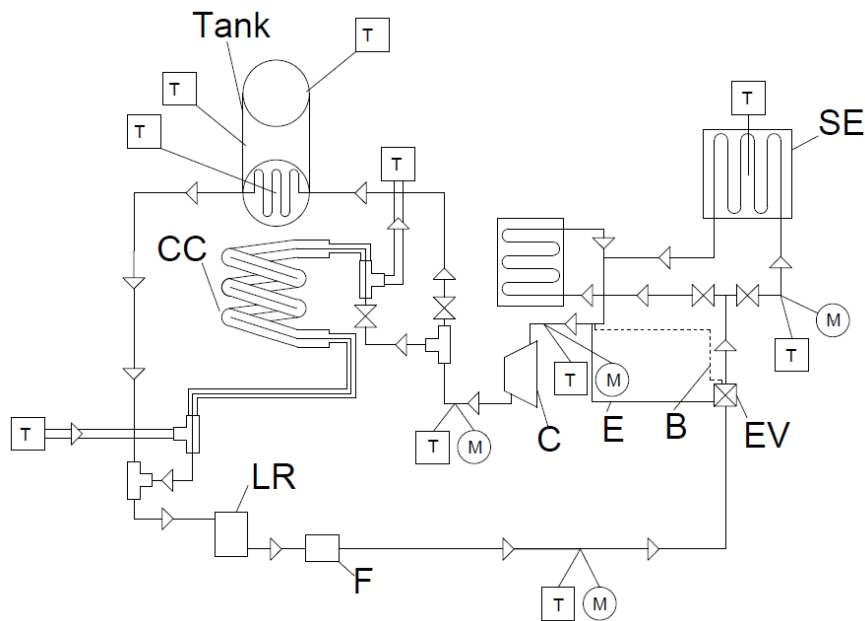


Figure 1. DX-SAHP diagram – SE: solar evaporator, EV: thermostatic expansion valve; C: compressor; CC: coaxial condenser; LR: liquid receiver, B: bulb, E: equalizer, F: filter dryer, M: bourdon gage, T: thermocouple

## 2. SYSTEM DESCRIPTION

Figure 1 depicts the schematic diagram of the heat pump in the present study. An 1/3 HP R134a hermetic compressor with volumetric displacement of 7.95 cm<sup>3</sup>, a thermostatic expansion valve, an unglazed flat-plate collector-evaporator (installed with a slope of 30°), a coaxial condenser (heating water from 30°C to 45°C), a 200 L isolated water reservoir and auxiliary components compose the DX-SAHP system. Figure 2 shows the prototype tested. Despite having an air-source evaporator and a condenser immersed in the tank, they did not partake in the tests. Bourdon gauges, Type K thermocouples and an analog energy meter were used to measure pressure, temperature and energy consumption respectively. Data acquisition system consisted of a USB-9162 - 24 bits for the thermocouples, a USB-6211 for the pyranometers, both connected in Labview® environment, which read and treated all data signals.

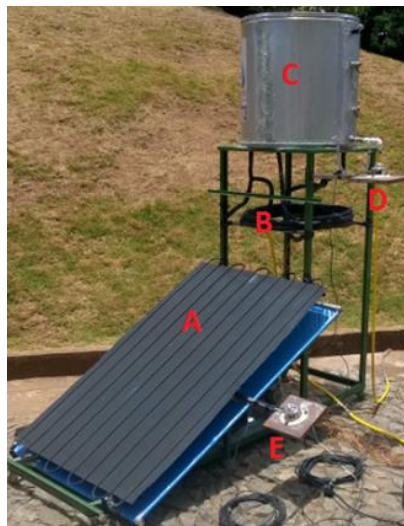


Figure 2. Overview of the heat pump – A: Solar evaporator, B: coaxial condenser, C: water reservoir, D: pyranometer (horizontal), E: pyranometer (evaporator's plane)



Figure 3. Coaxial condenser

The evaporator coil is made of copper with internal and external diameters of 8.73 mm and 9.53 mm respectively. Straight tubes total length is 16.0 m, while the return bends outside the plate totals 1.28 m. The unglazed plate was made of aluminum, 1.03 m wide, 1.60 m long and 1 mm thick. The plate received black painting to maximize irradiation absorption. An emissivity of 0.95 was measured using a thermographic camera with gray body behavior for absorptivity. Two pyranometers measured the flux of radiation in the solar evaporator, one horizontal and one inclined 30° (same plane of the collector).

Figure 3 highlights the condenser. It is 5.5 m long and 92.1 mm high, and spirals in 2.7 turns with a diameter of 0.65 m. The inner tube has internal and external diameters of 4.76 mm and 6.35 mm, while the outer tube has diameters of 11.11 mm and 12.70 mm respectively. Both tubes are made of copper. R134a flows into the central pipe while water flows countercurrent into the annular space. A 9 mm thick polyethylene insulation tube covered the condenser with a thermal conductivity of 0.038 W/m.K, to reduce heat losses to the environment. Table 1 shows the measurement uncertainties of the measuring instruments used.

Table 1. Uncertainty of the measurement instruments

Measuring instrument	Uncertainty
Type K Thermocouple	± 1 °C
Bourdon gauge (low pressure)	± 0,1 bar
Bourdon gauge (high pressure)	± 0,35 kgf/cm <sup>2</sup>
Pyranometer	± 5%
Energy meter	± 1%
Beaker	± 50 ml

### 3. METHODOLOGY

A test was conducted on 01/26/2016 (summer) starting at 10:30. Prior to it, the water flow was manually set so that the temperature at the inlet of the tank was 45°C. This flow rate was measured by timing the time required to fill a 1 L beaker with circulating water in the system. Three measurements were taken and the mean value was adopted. Although not performed at the beginning of the test, the flow rate varied very little.

The assay contained 16 measurements performed at fixed intervals of 15 minutes. At each measurement interval, the solar irradiance at the evaporator, the temperature and pressure at the inlet and outlet of each component, the water temperature at the inlet and outlet of the coaxial condenser, the ambient temperature, the average plate temperature, and the electric power consumed by the compressor were measured. The test stopped when the tank was filled with 200 L of water.

The machine used had only one passage for water; thus, the principle of continuity ensures that the mass flow of water in all components is equal.

Equation (1) provides an energy balance for the water in the condenser. The 'w' subscribe stands for water, while the inlet and outlet refers to the condenser.

$$\dot{Q}_w = \dot{m}_w c_p (T_{w,outlet} - T_{w,inlet}) \quad (1)$$

This equation gives the heat transfer rate received by the water in the passage through the condenser. The specific heat,  $c_p$ , was evaluated at the average inlet and outlet temperatures of the condenser.

Equation (2) provides the compression work. The interval of measurement,  $\Delta t$ , equals 15 minutes.

$$\dot{W} = \Delta E / \Delta t \quad (2)$$

The real COP is defined as the amount of energy absorbed by the water by the amount of energy expended. Both measured quantities. The energy absorbed by the water is the product of the heating capacity by the interval of measurement, in this case, 15 minutes.

$$COP = \frac{\dot{Q}_w \cdot \Delta t}{\Delta E} \quad (3)$$

#### 4. RESULTS

Test started at 10:30, for sixteen measurements. The water flow rate adjusted before the test was 52.7 L / h, with few fluctuations in the on-going trial. Figure 4 shows the water temperature at inlet and outlet of the condenser. The water heated from an average temperature of 29.1 °C to an average temperature of 45.2 °C. The mean air temperature was 32.7 °C while the average plate temperature was 34.0 °C. The mean heating capacity was 1093.4 W while the average COP was 2.66.

Figure 5 shows the air and evaporator's plate temperature profile. The ambient temperature rose throughout the test, starting at 31.0 °C, to a peak of 34.8 °C in 195 minutes of testing, consistent since the temperature peak normally occur at 1:30 p.m. or 2:00 p.m. The temperature of the plate also presented a growth profile, however with higher temperature oscillations and solar irradiation dependence. With approximately 120 min of test, the sky became cloudy, which greatly reduced the incidence of irradiation in the plane of the plate, with according reduction in the temperature of the solar evaporator. Figure 6 shows the irradiation profile. The irradiation grows continuously and has peak at noon; however, the period of 120 to 150 min, which would present the highest irradiation, was compromised due to the cloudy sky.

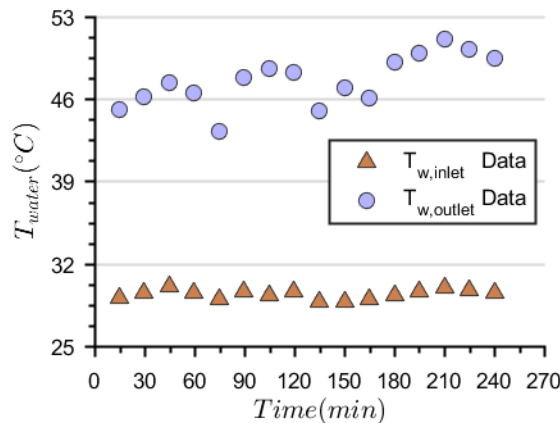


Figure 4. Water temperature at the inlet and outlet of the condenser

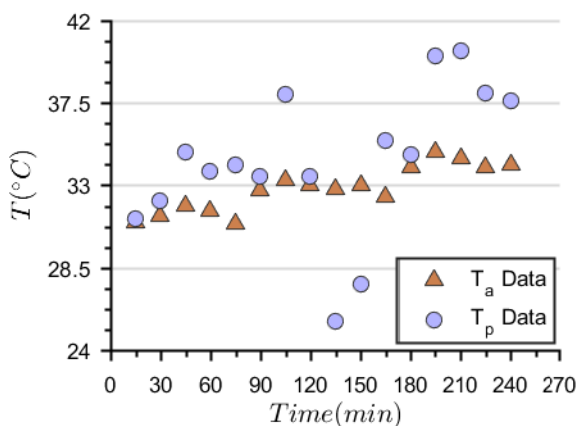


Figure 5. Air and plate temperatures

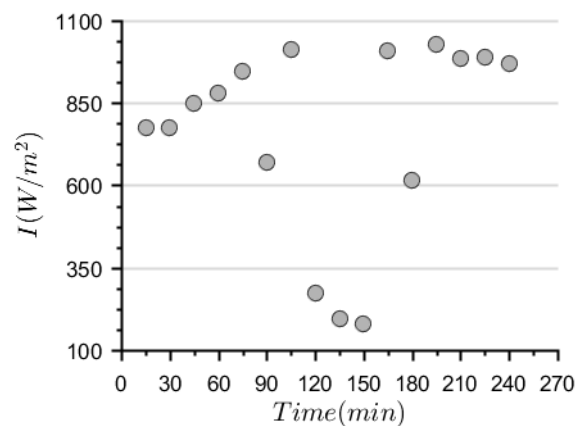


Figure 6. Irradiation profile

Figure 6 and 7 show the compressor power and the heating capacity. Compressor power has grown steadily over time due to the increment in condensation temperature, which occurred because of the increase in ambient temperature. Despite this raise, the heating capacity increased more, which translated into COP gain, as shown in Fig. 8. This increase in COP, despite the increase in condensation temperature, was possible because the evaporation temperature and irradiation increased during test. Figure 9 shows the dependence of the COP with the ambient temperature and temperature of the solar evaporator, confirming that the increase in temperature generates an increase in COP. Figure 10 shows the dependence of COP with solar irradiation, indicating that higher radiations correspond to higher COPs. Although the relative influence of the irradiation on the evaporator was not investigated directly in this paper, the low irradiance data corresponded to smaller values of COP, demonstrating its influence on the thermal performance of the heat pump.

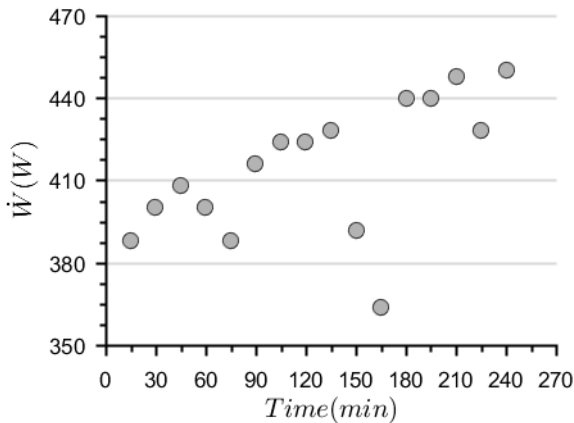


Figure 6. Compressor power

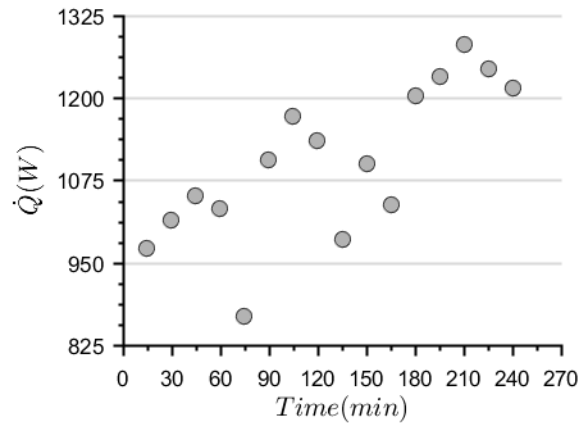


Figure 7. Heating capacity

Figure 6 and 7 show the compressor power and the heating capacity. Compressor power has grown steadily over time due to the increment in condensation temperature, which occurred because of the increase in ambient temperature. Despite this raise, the heating capacity increased more, which translated into COP gain, as shown in Fig. 8. This increase in COP, despite the increase in condensation temperature, was possible because the evaporation temperature and irradiation increased during test. Figure 9 shows the dependence of the COP with the ambient temperature and temperature of the solar evaporator, confirming that the increase in temperature generates an increase in COP. Figure 10 shows the dependence of COP with solar irradiation, indicating that higher radiations correspond to higher COPs. Although the relative influence of the irradiation on the evaporator was not investigated directly in this paper, the low irradiance data corresponded to smaller values of COP, demonstrating its influence on the thermal performance of the heat pump.

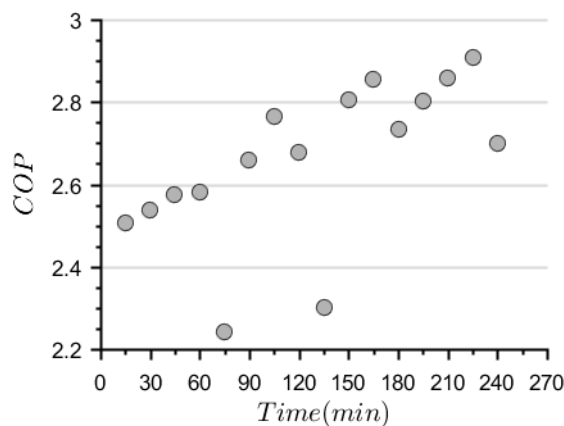


Figure 8. COP x time



## **8. RESPONSIBILITY NOTICE**

The authors are the only responsible for the printed material included in this paper.